Journal of Gerontology: BIOLOGICAL SCIENCES
Cite journal as: J Gerontol A Biol Sci Med Sci
2009. Vol. 64A, No. 7, 731–739
doi:10.1093/gerona/glp040

Advance Access publication on April 9, 2009

Use of Senescence-Accelerated Mouse Model in Bleomycin-Induced Lung Injury Suggests That Bone Marrow–Derived Cells Can Alter the Outcome of Lung Injury in Aged Mice

Jianguo Xu,[1,2] Edilson T. Gonzalez,[1,2] Smita S. Iyer,[1,2] Valerie Mac,[1,2] Ana L. Mora,[1,2,3] Roy L. Sutliff,[1] Alana Reed,[1] Kenneth L. Brigham,[1,2,3] Patricia Kelly,[1,2] and Mauricio Rojas[1,2,3]

[1]Division of Pulmonary, Allergy and Critical Care Medicine, [2]Center for Translational Research in the Lung, and [3]McKelvey Center for Lung Transplantation, Department of Medicine, Emory University School of Medicine, Atlanta, Georgia.

The incidence of pulmonary fibrosis increases with age. Studies from our group have implicated circulating progenitor cells, termed fibrocytes, in lung fibrosis. In this study, we investigate whether the preceding determinants of inflammation and fibrosis were augmented with aging. We compared responses to intratracheal bleomycin in senescence-accelerated prone mice (SAMP), with responses in age-matched control senescence-accelerated resistant mice (SAMR). SAMP mice demonstrated an exaggerated inflammatory response as evidenced by lung histology. Bleomycin-induced fibrosis was significantly higher in SAMP mice compared with SAMR controls. Consistent with fibrotic changes in the lung, SAMP mice expressed higher levels of transforming growth factor-β1 in the lung. Furthermore, SAMP mice showed higher numbers of fibrocytes and higher levels of stromal cell–derived factor-1 in the peripheral blood. This study provides the novel observation that apart from increases in inflammatory and fibrotic factors in response to injury, the increased mobilization of fibrocytes may be involved in age-related susceptibility to lung fibrosis.

Key Words: Lung—Senescence—Bone marrow—Mice.

AGING is characterized as a progressive decline in tissue and organ function, accompanied by increased free radical damage (1), mitochondrial dysfunction (2), endocrine imbalance (3), and genome instability (4). Aging is also associated with a decline in immunity described as immunosenescence, a well-recognized phenomenon in humans and animals (5). Especially relevant to the fibrotic response, normal aging is associated with a shift in T lymphocytes from a predominantly T-helper (T_H) 1 phenotype to a predominantly T_H2 phenotype by increasing the production of interleukin (IL)-4, IL-5, IL-10, and IL-13, which are responsible for strong profibrotic response and transforming growth factor (TGF)-β1 production.

Several recent studies have documented differences in bone marrow–derived stem cell (BMDMSC) performance between young and old animals. Administration of endothelial progenitor cells from young, but not from old, mice restored pathways critical for cardiac angiogenesis in senescent mice without prior bone marrow (BM) suppression (6). Rauscher and associates (7) demonstrated that chronic treatment with BM-derived progenitor cells from young nonatherosclerotic $ApoE^{-/-}$ mice prevented the progression of atherosclerosis in aged $ApoE^{-/-}$ mice despite persistent hypercholesterolemia . In a remarkable study, Conboy and coworkers (8) demonstrated that heterochronic parabiotic mice (two mice, one old and one young, surgically joined with shared circulatory systems) restored age-related loss of stem cell capacity in muscle, blood, and liver in the older member of the pair.

The senescence-accelerated mouse (SAM) is a commonly used model for studying physiological and pathological responses during aging. The SAM strain is derived from the AKR/J strain of mice by continuous brother–sister mating selected for a phenotype toward either accelerated senescence or resistance senescence. There are nine major senescence-accelerated prone mouse (SAMP, P) strains and three major senescence-accelerated resistant mouse (SAMR, R) strains (9). The P8 strain of SAMP (SAMP8) shows spontaneous learning and memory defects at 2 months of age, which deteriorate with aging (10). SAMP8 mice are also prone to amyloid deposition, cataracts, osteoporosis, degenerative joint disease, decreased immune responses, increased lordokyphosis, and various other hallmarks of aging (11).

Although both the incidence and the severity of acute lung injury and fibrotic lung disease increase with age, there is relatively little known about the mechanisms by which aging increases susceptibility to these lung diseases. Research from our lab and others has shown that BMDMSCs play a critical role in lung injury and fibrosis. We hypothesize that aging affects the response of BMDMSCs to lung injury. In addition to addressing a fundamental biologic mechanism, the study provides a rationale for interventions that can be tested in animal models and could eventually be applicable to humans.

Methods

Animal Maintenance

Six- and 12-month-old female SAMP8 and SAMR1 mice were purchased from Harlan (Indianapolis, IN) and bred in the Department of Animal Resources, Emory University. All animal experiments were performed in accordance with the Emory University Institutional Animal Care and Use Committee.

Bleomycin Administration

Mice were anesthetized by isofluorane inhalation and the trachea was exposed using sterile technique. About 3.6 U/kg bleomycin (Sigma-Aldrich, St Louis, MO) in 75 μL of phosphate-buffered saline (PBS) or PBS vehicle was injected into the tracheal lumen. After inoculation, the incision was closed and the animals were allowed to recover. Seven and 14 days after bleomycin injection, the mice were killed by isofluorane inhalation and lungs harvested and inflated to a constant pressure of 20 cc of water.

Enzyme-Linked Immunosorbent Assay for Serum Stromal Cell–Derived Factor-1

Peripheral blood was collected from the retro orbital sinus, and serum was collected after clotting. A quantitative immunoassay was used for serum stromal cell–derived factor-1 (SDF-1) measurement, according to the manufacturer's protocol (R&D Systems, Minneapolis, MN).

Western Blot for Detecting TGF-β1, and Collagens I and IV

Lung samples (20 μg protein per lane) were run on 10% sodium dodecyl sulfate-polyacrylamide gel electrophoresis (SDS-PAGE) gels (Invitrogen, Carlsbad, CA) for 1 hour at 150 V and then transferred to nitrocellulose membranes. The blots were blocked in "blot buffer" (2% nonfat dry milk, 0.1% Tween 20, 50 mM NaCl, 10 mM Hepes, pH 7.4) for at least 30 minutes. Blots were then incubated with a rabbit anti-TGF-β, collagen IV (Santa Cruz Biotechnology, Santa Cruz, CA), collagen I (Millipore, Billerica, MA) or a mouse anti-β-actin antibody (Sigma). The blots were then washed three times with 10 mL of blot buffer and incubated for 1 hour at room temperature with a horseradish peroxidase–conjugated anti-rabbit or anti-mouse secondary antibody (Amersham Biosciences, Pittsburgh, PA) in blot buffer. Finally, the blots were washed three more times with 10 mL of blot buffer and visualized via enzyme-linked chemiluminescence using the SuperSignal West Pico kit (Pierce Biotechnology, Rockford, IL).

Fluorescence-Activated Cell Sorting

Five hundred microliters of whole blood was collected from a single mouse with heparinized microtubes. Red blood cells were lysed using ammonium chloride potassium lysis buffer. Cells were pelleted and resuspended with fluorescence-activated cell sorting (FACS) buffer (3% bovine serum albumin and 0.1% sodium azide in PBS) to a concentration of 5×10^6 cells/mL. Cells were surface stained with fluorescein isothiocyanate-conjugated anti-mouse-CD45 (BD Biosciences, Mountain View, CA) and phycoerythrin-anti-mouse CXCR4 (BD Biosciences). Cells were permeabilized with Cytofix/Cytoperm (BD Biosciences) and stained with a rabbit anti-collagen I antibody, followed by allophycocyanin-conjugated goat anti-rabbit IgG. Isotype antibody controls were performed for all of the antibodies used and were added either before or after cell permeabilization, depending on whether the antigen was intracellular or extracellular. Both labeled and unlabeled samples were then analyzed on a FACSCalibur (Becton Dickinson, Mountain View, CA). Flow cytometry data were analyzed using the FlowJo 7.2.5 software (Tree Star Inc, San Carlos, CA).

Hydroxyproline Assay

Hydroxyproline content in whole mouse lungs was used to quantify lung collagen content and was measured colorimetrically by the method described previously, with modifications (12). At the time of killing, all lobes of the lung were removed and the extrapulmonary airways and blood vessels excised and discarded. The lung parenchyma was homogenized in 1.0 mL of PBS, after which 1.0 mL of 12N HCl was added, and the samples were hydrolyzed at 110°C for 24 hours. Five microliters of each sample was mixed with 5 μL of citrate–acetate buffer (5% citric acid, 1.2% glacial acetic acid, 7.25% sodium acetate, and 3.4% sodium hydroxide). One hundred microliters of chloramine-T solution (1.4% chloramine-T, 10% N-propanol, and 80% citrate–acetate buffer) was added, and the mixture was incubated for 20 minutes at room temperature. Ehrlich's solution was added and the samples were incubated at 65°C for 18 minutes. Absorbance was measured at 550 nm. A standard curve was generated for each experiment using a hydroxyproline standard. Results were expressed as micrograms of hydroxyproline per lung.

Migration Assay

Fresh BM cells were isolated by flushing PBS through the end of both femurs and washing once with Dulbecco's modified eagle medium (DMEM) containing penicillin–streptomycin. Cells were plated at 10^6 cells per 100-mm cell culture dish in DMEM containing 20% fetal calf serum, nonessential amino acids, pyruvate, the antibiotic penicillin at 200 IU/mL, and streptomycin at 250 μm/mL, and cultured at 5% CO_2 atmosphere. After 48 hours, nonadherent cells were removed and fresh media was added to the culture. At day 7, cells were harvested by treating the culture with 0.25% trypsin for 5 minutes, followed by gentle scraping to remove cells. BMDMSCs were purified by passing a MACS system column twice (Miltenyi Biotec, Auburn, CA) to eliminate CD45+ and CD11b+ cells. The resulting BMDMSCs were more than 99% CD45−. Migration of

BMDMSCs was determined by incubation in transwells (Corning, Corning, NY). Cells were resuspended in modified Dulbecco's medium, and 1×10^5 cells were loaded into the 8-μm upper chamber of transwell inserts. Recombinant SDF-1α at 200 ng/mL (R&D Systems) was added to the lower chamber. Transmigrated cells were collected by centrifugation, following a 2-hour incubation at 37°C. Cells in the lower well were quantified using a hemocytometer.

BMDMSC Differentiation

For chondrogenesis studies, 250,000 cells were placed in a 15-mL polypropylene tube (Becton Dickinson) and centrifuged for 10 minutes. The pellet was cultured in chondrogenesis medium (high-glucose Dulbecco's modified Eagle's medium [Invitrogen]) supplemented with 10 ng/mL TGF-β3 (R&D Systems), 10^{-7} M dexamethasone (Sigma), 50 μg/mL ascorbate-2-phosphate, 40 μg/mL proline, 100 μg/mL pyruvate, and 50 mg/mL ITS+ Premix (Becton Dickinson). The pellets were embedded in paraffin, cut into 5-μm sections, and stained with alcian blue and visualized by microscopy. For adipogenesis experiments, 10^4 cells were plated in 60-cm^2 dishes and cultured in complete medium for 3 days. The medium was then switched to adipogenic medium, which consisted of complete medium supplemented with 10^7 M dexamethasone, 0.5 mM isobutyl-1-methyl xanthine (Sigma-Aldrich), and 50 μM indomethacin (Wako, Tokyo, Japan) for an additional 21 days. The adipogenic cultures were fixed in 4% paraformaldehyde and stained with fresh oil red O solution, and oil red O–positive colonies were counted. Colonies that were less than 2 mm in diameter or were stained only faintly were not included in the analyses.

Histology and Immunohistochemistry

For each experimental time point in the study, there were five mice per group. After inflation to a pressure of 20 cc of water and fixation with 4% paraformaldehyde for 24 hours, lung tissues were paraffin embedded, sectioned, and stained with hematoxylin and eosin (H&E) for routine histological examination. Masson's trichrome staining was used to delineate collagen content.

Statistical Methods

For comparisons between groups, paired or unpaired *t* tests, and one-way and two-way analysis of variance tests were used (p values <.05 were considered significant). GraphPad Prism and GraphPad InStat were used to calculate the statistics.

Results

SAMP8 Mice Were More Susceptible to Bleomycin-Induced Lung Fibrosis as Compared With SAMR1 Mice

To determine the effects of aging on bleomycin-induced lung injury, 12-month-old SAMP8 and SAMR1 mice were treated with a single intratracheal instillation of 3.6 U/kg bleomycin or PBS. Fourteen days after bleomycin administration, lung samples were harvested. H&E-stained lung sections from the pro-senescence SAMP8 mice showed loss of normal pulmonary architecture, with massive inflammatory cell infiltration and interstitial fibrosis. In contrast, lungs from the senescence-resistant SAMR1 mice collected at the same time after bleomycin administration showed mild inflammation and fibrosis (Figure 1A). Lungs from SAMP8 and SAMR1 mice treated with saline solution had normal architecture. To determine the extent of lung fibrosis, sections were stained with Masson's trichrome, which reveals an extensive collagen deposition in the extracellular space. Collagen content in lungs from both groups of mice was quantified by measuring hydroxyproline content (Figure 1B). Biochemical measurements of lung collagen content were consistent with the histological sections, showing significant increase in hydroxyproline in bleomycin-treated SAMP8 compared with the SAMR1 mice.

To corroborate the increase in collagen content in the lungs of SAMP8 by histology and hydroxyproline content, collagen I and collagen IV content was determined by western blot (Figure 2). We observed an increase in the amount of collagen I in both groups after bleomycin, but the increase was more prominent in SAMP8 group. When the content of collagen IV was determined, it was only detected in the lungs obtained from SAMP8 mice treated with bleomycin.

TGF-β1 Expression Increases in the Lungs of SAMP8 Mice After Bleomycin Instillation

TGF-β1 is a critical mediator of bleomycin-induced pulmonary fibrosis (13). A high-dose adenoviral transfer of TGF-β1 causes a progressive fibrotic response in the lung in vivo and an idiopathic pulmonary fibrosis (IPF)-like disease with fibroblastic foci in an explant culture system (14). To determine whether TGF-β1 is involved in lung fibrosis of senescent mice, lung TGF-β1 levels in bleomycin-treated SAMP8 and SAMR1 were determined by western blot. Results showed that at basal state, SAMP8 mice have higher active TGF-β1 levels than SAMR1 mice (Figure 3A). Furthermore, bleomycin treatment increased active TGF-β1 levels in both SAMP8 and SAMR1 mice, although higher increase was observed in SAMP8 mice. Figure 3B summarizes quantitative data from the blots of inactive and active TGF-β1.

Increased Fibrocytes in SAMP8 Mice After Bleomycin Treatment

One of proposed sources of fibroblast in pulmonary fibrosis is the recruitment of BM-derived fibroblast progenitor cells, also called fibrocytes (15). To determine whether fibrocytes play a role in lung fibrosis of senescent mice, 12-month-old SAMP8 and SAMR1 mice were treated intratracheally

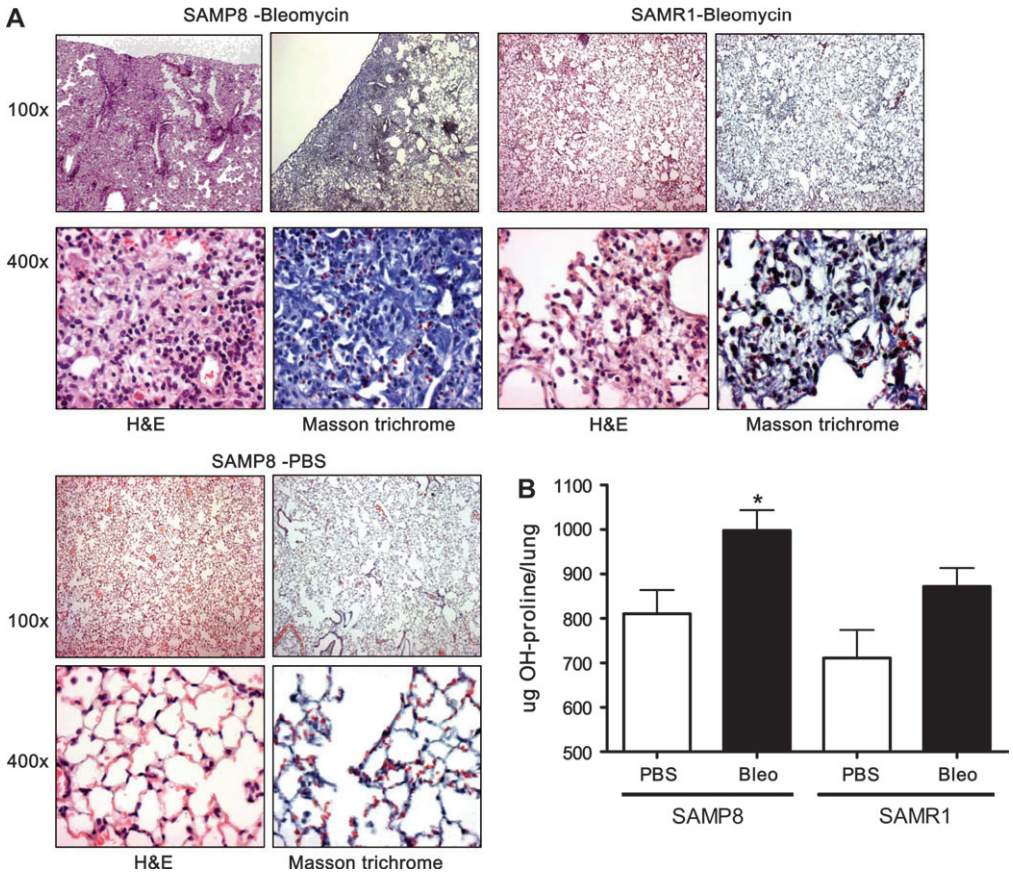

Figure 1. Twelve-month-old SAMP8 and SAMR1 mice were administered with 3.6 U/kg of bleomycin intratracheally. Fourteen days after bleomycin or phosphate-buffered saline treatment, lung samples were harvested and fixed with 4% paraformaldehyde. (**A**) Tissue sections were stained with hematoxylin and eosin and Masson's trichrome. Pictures were taken under 100× and 400× magnification. (**B**) To quantify the collagen content of lung tissue, the content of hydroxyproline was determined. We observed a significantly higher ($p < .001$) collagen content in the 12-month SAMP8 mice treated with bleomycin than in SAMR1 mice after bleomycin. *Note:* SAMP = senescence-accelerated prone mice; SAMR = senescence-accelerated resistant mice. $n = 17–22$.

with bleomycin. Seven days after the bleomycin instillation, peripheral blood samples were collected and assayed for $CXCR4^+CD45^+Col\ I^+$, which are the hallmark markers for fibrocytes. As shown in Figure 4, seven days after intratracheal instillation of bleomycin, the percentage of fibrocytes circulating in the blood of SAMP8 mice was significantly higher compared with that in SAMR1 mice (2.3% vs 0.1%, $p < .01$). We did not detect fibrocytes in circulation on the PBS-treated mice.

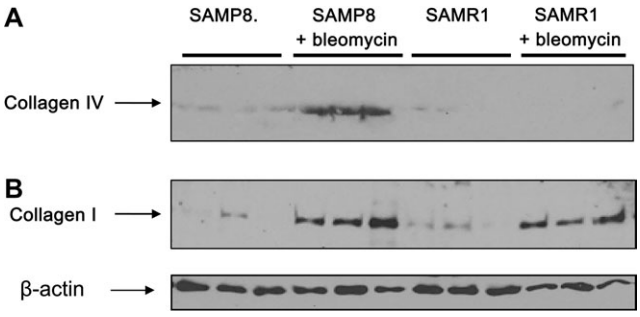

Figure 2. We confirmed the increase in collagen content in the lungs of the mice treated with bleomycin by western blot. Lung lysates (20 μg protein per lane from 6-month-old SAMP8 and SAMR1 mice) were run by using 7% sodium dodecyl sulfate-polyacrylamide gel electrophoresis and then transferred to nitrocellulose membranes, and collagens I and IV was determined by using specific antibodies. There is an important increase in the levels of collagen I in both groups treated with bleomycin but higher in the SAMP8 group. When the content of collagen IV was determined, we detected increase in the SAMP8 group. *Note:* SAMP = senescence-accelerated prone mice; SAMR = senescence-accelerated resistant mice.

Altered SDF-1 Levels and SDF-1-Mediated BMDMSC Migration in SAMP8 Mice

SDF-1 has been shown to play a role in bleomycin-induced lung fibrosis, possibly by attracting different types of BM-derived cells, including fibrocytes and BMDMSCs, to the site of lung injury (16). To determine if there was an altered SDF-1 response in SAMP8 mice, female 6- and 12-month-old SAMP8 mice were treated with one dose of either bleomycin or PBS vehicle intratracheally, and serum samples were harvested at days 7 and 14. Figure 5A summarizes serum concentrations of SDF-1 in SAMP8 mice, determined by enzyme-linked immunosorbent assay over the course of the bleomycin response. On day 7, serum SDF-1 levels in the 6-month-old SAMP8 mice were significantly lower

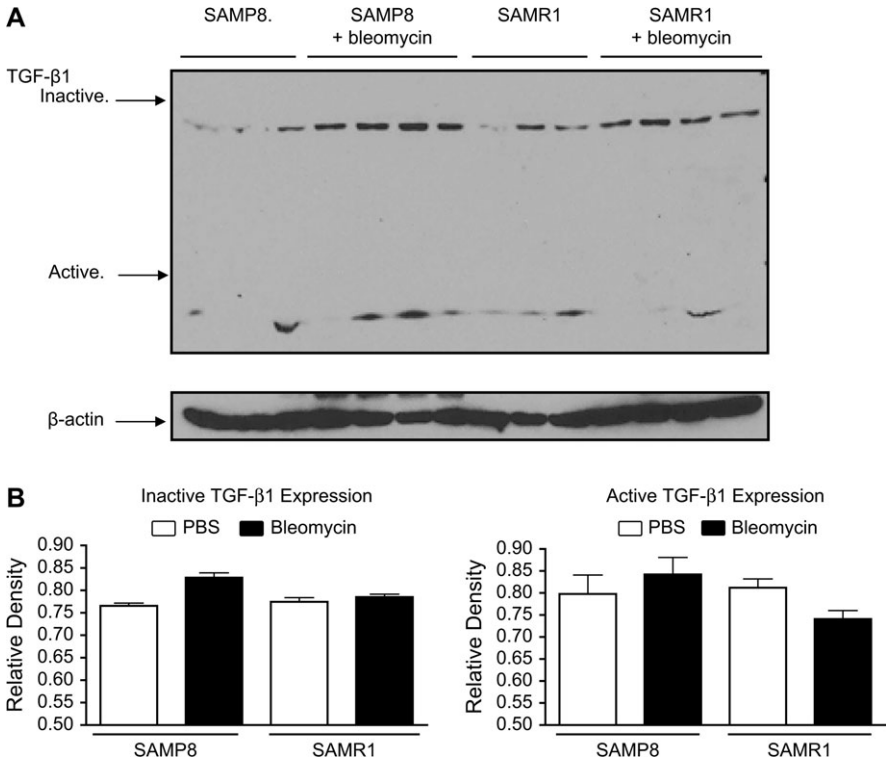

Figure 3. Western blot was used for detecting lung TGF-β1. Lung lysates (20 μg protein per lane from 6-month-old SAMP8 and SAMR1 mice) were run by using 10% sodium dodecyl sulfate-polyacrylamide gel electrophoresis and then transferred to nitrocellulose membranes. (**A**) At basal state, SAMP8 mice had higher active TGF-β1 levels than SAMR1 mice. Additionally, bleomycin treatment increased active TGF-β1 levels in both SAMP8 and SAMR1 mice, although higher increase was observed in SAMP8 mice. (**B**) Quantitation of active and inactive TGF-β1 levels from western blot by densitometry. Mean value of β-actin levels was designated as 1 for each group. Values represent mean ± standard error. *Notes:* SAMP = senescence-accelerated prone mice; SAMR = senescence-accelerated resistant mice; TGF = transforming growth factor. $n = 4$. *$p < .05$.

compared with those in the 12-month-old SAMP8 mice. A similar reduction in SDF-1 was observed at day 14 after bleomycin treatment. To explore the roles of SDF-1/CXCR4 axis in recruitment of BMDMSCs to injured lungs, we performed an in vitro migration assay using purified BMDMSCs, from SAMP8 and SAMR1 mice; the data are summarized in Figure 5B. SDF-1 induced strong chemotactic migration of BMDMSCs in SAMR1 mice (an approximate 12-fold increase over control, $p < .01$), whereas migration was significantly minor in SAMP8 mice (an approximate threefold increase over control, $p < .01$).

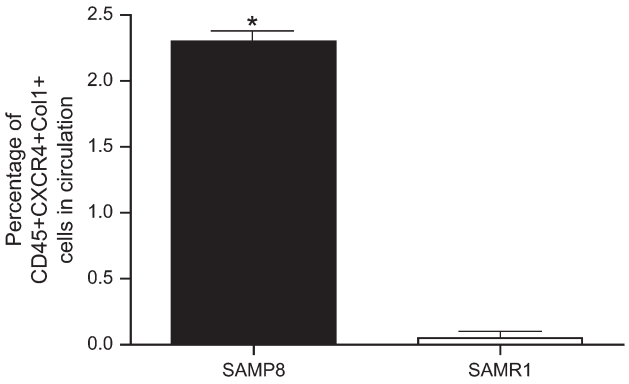

Figure 4. FACS analysis of fibrocytes ($CXCR4^+CD45^+Col\ I^+$) in peripheral blood after bleomycin treatment. Six-month-old SAMP8 and SAMR1 mice were administered with 4 U/kg of bleomycin intratracheally. Seven days after the bleomycin treatment, peripheral blood samples were analyzed for $CXCR4^+$, $CD45^+$, and Col I^+. Flow cytometry data showed higher number of fibrocytes in circulation in samples obtained from SAMP8 mice. Values represent mean ± standard error. *Notes:* FACS = fluorescence-activated cell sorting; SAMP = senescence-accelerated prone mice; SAMR = senescence-accelerated resistant mice. $n = 3$. *$p < .001$.

Differentiation of SAMP8 and SAMR1 BMDMSCs Into Different Cell Types

To determine if there was a difference in the potential of the SAMP8 and SAMR1 BMDMSCs to differentiate into different cell types, BMDMSCs from 12-month-old SAMP8 and SAMR1 mice were isolated and cultured for 7 days (Figure 6). BMDMSCs were then placed in pellet culture and treated with adipogenic or chondrogenic media for 2 weeks. Adipocytes and chondrocytes were examined by oil red O staining and alcian blue staining, respectively. The results showed that BMDMSCs from SAMP8 mice are more prone to differentiate into adipocytes than those from SAMR1 mice (10.9% vs 5.4%). BMDMSCs from SAMP8 mice show a decrease in their ability to differentiate into

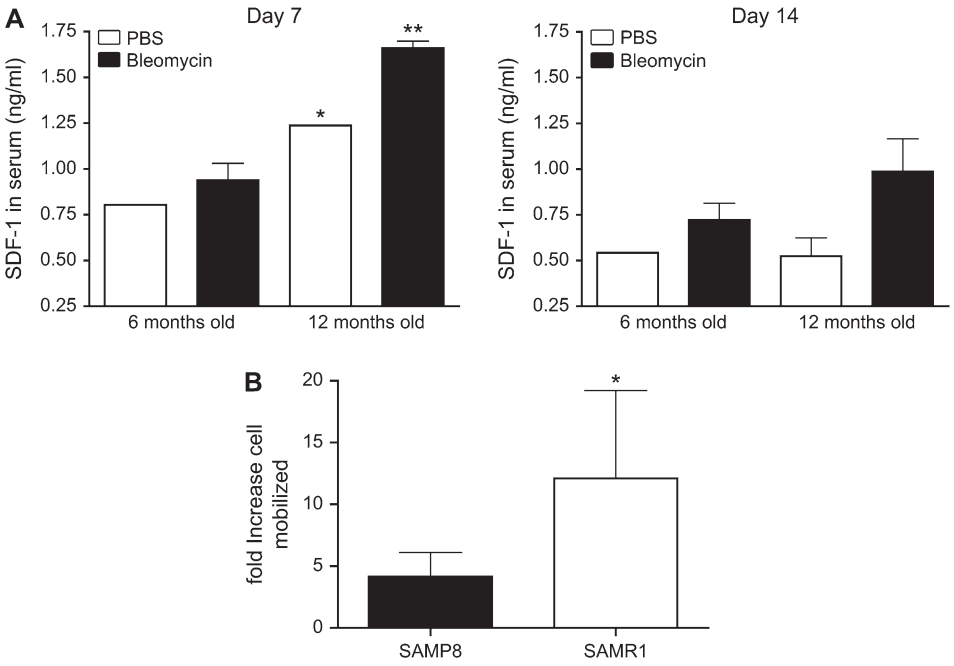

Figure 5. Expression of SDF-1 increases with age but the ability of BMDMSCs to respond decreases. (**A**) SAMP8 mice were intratracheally treated with 4 U/kg of bleomycin at the moment of sacrifice 7 and 14 days after injury, and then, samples of peripheral blood were collected. Levels of SDF-1 were measured by enzyme-linked immunosorbent assay and concentrations expressed in ng/mL. There were significant differences in the SDF-1 levels in serum between the 6-month and 12-month samples. (**B**) To evaluate the ability of BMDMSCs to respond to SDF-1, BMDMSCs were obtained from 12-month-old SAMP8 and SAMR1 mice. Cells were exposed for 2 hours to 200 ng/mL of SDF-1 and the number of cells that migrated was quantified using a hemocytometer. Values represent mean ± standard error. *Notes:* BMDMSC = bone marrow–derived stem cell; SAMP = senescence-accelerated prone mice; SAMR = senescence-accelerated resistant mice; SDF = stromal cell–derived factor. $n = 4$. *$p < .05$ and **$p < .001$.

chondrocytes compared with BMDMSCs from SAMR1 controls (1.6% vs 7.5%).

Discussion

IPF is considered a disease of older people. Incidence increases with age, and in most cases, the age of onset is 60–70 years (17). In fact, a clinical picture consistent with this diagnosis is considered suspect if the patient is younger than 50 years. In patients with asbestos exposure, development of asbestos-related lung fibrosis increases with age even when controlled for amount of exposure (18). Animal studies document increased susceptibility of the aged lung to fibrotic stimuli. For example, relaxin-deficient mice develop an age-related form of pulmonary fibrosis (19), and lung fibrosis induced by cigarette smoke exposure is greater in old mice (8–10 months) than young mice (2 months (20)).

In this study, we used SAMP and SAMR to investigate the effects of aging on bleomycin-induced lung fibrosis. We found that SAMP8 are more prone to bleomycin-induced lung injury, as well as increased TGF-β1 levels. SAMP8 mice have elevated SDF-1 levels that increase with age. However, when we evaluated the ability of SAMP8 BMDMSCs to respond to SDF-1, we observed a reduction in SDF-1-induced cell migration compared with SAMR1 mice. BMDMSCs from SAMP8 mice have an increased tendency to transform to adipocytes and a reduced tendency to transform to chondrocytes compared with SAMR1. These data are consistent with the hypothesis that aging mice are more prone to lung injury. This may be mediated by a defect in the type of cells recruited into the lung. A high number of fibrocytes and a lower number of BMDMSCs with a poor ability to differentiate into any other type of cell could result in an altered inflammatory response and affect lung repair.

Chemokines are classified into two groups, C-C chemokines and C-X-C chemokines. SDF-1 is a member of the C-X-C chemokine subfamily and the only known ligand for the G protein–coupled receptor, CXCR4, a coreceptor for human immunodeficiency virus (21). The primary structure of SDF-1 is remarkably conserved across species, with only one amino acid difference between the human and mouse proteins. Two isoforms of SDF-1, SDF-1α and SDF-1β, differ by only four amino acids at the C-terminus and are generated from a single gene by differential RNA splicing (22). SDF-1 has several biologic roles. In addition to controlling cell motility, SDF-1 regulates cell proliferation, induces cell cycle progression, and acts as a survival factor for both human and murine stem cells (23,24). Knockout murine embryos lacking SDF-1 or its receptor CXCR4 show multiple lethal defects, including impaired BM lymphoid and myeloid hematopoiesis (25,26). These defects can be partially corrected by forced expression of SDF-1 in the fetal BM endothelium of SDF-1 knockout mice (27). In contrast to

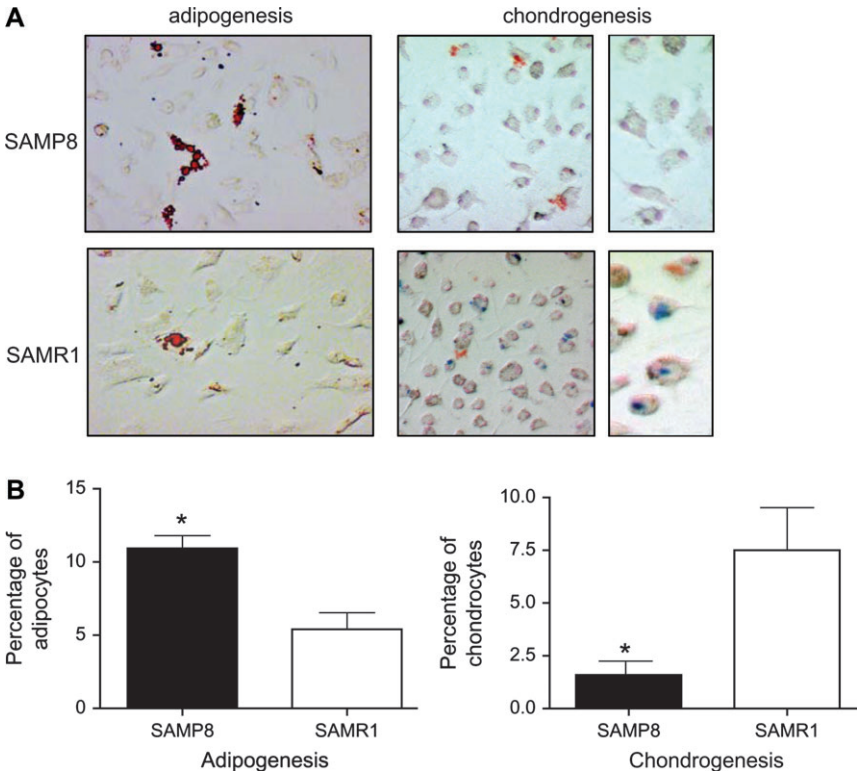

Figure 6. BMDMSCs obtained from bone marrow of SAMP8 mice had a decreased ability to differentiate into chondrocytes. To demonstrate if the potential of BMDMSCs to differentiate is modified with age, BMDMSCs obtained from 12-month-old SAMP8 and SAMR1 mice were cultured in a chondrogenic basal media and adipogenic media for 14 days. Transformed cells were visualized by staining the cells: alcian blue for chondrocytes and oil red O staining for adipocytes. (**A**) Positive transformed cells stained blue (arrow) under light microscopy, 20× and 100× magnification. (**B**) The number of transformed cells was determined by counting the number of positive of cells for every 100 nucleus. *Notes:* BMDMSC = bone marrow–derived stem cell; SAMP = senescence-accelerated prone mice; SAMR = senescence-accelerated resistant mice. $n = 4$. $^*p < .01$.

other proinflammatory chemokines, SDF-1 is constitutively produced in many organs including the human BM (28). Both, BMDMSCs and fibrocytes can express the SDF-1 receptor, CXCR4 (29).

SDF-1 is a powerful reported chemoattractant for BM-derived cells (30). Cells are mobilized into peripheral blood and injured tissue in response to an SDF-1 gradient established by an increased expression of SDF-1 in injured tissue (31,32). For example, SDF-1 is reported to stimulate recruitment of progenitor cells to ischemic tissue (33,34). It was hypothesized that SDF-1 is regulated in limb ischemic tissues and that ischemia-associated hypoxia causes an imbalance between plasma and BM SDF-1 concentration, thereby promoting mobilization of stem cells from the BM (35). In addition, overexpression of SDF-1 augmented stem cell homing and incorporation into ischemic tissues (36). Irradiation or inflammation and hepatic injury are reported to increase SDF-1 levels, as well as CXCR4 expression and SDF-1-mediated recruitment of hematopoietic progenitors to the liver (37). In addition to its role as a stem cell chemoattractant, SDF-1 also activates matrix metalloproteinase (MMP)-9, which may contribute to mobilization and recruitment of BM cells (38). It has been demonstrated that SDF-1 induces the expression and release of MMP-9 by purified mature polyploid human megakaryocytes and an adeno-CXCR4-infected megakaryocytic cell line. Neutralizing the antibody to MMP-9, but not MMP-2, blocked SDF-1-induced migration of megakaryocytes through reconstituted basement membrane (38).

Two strains of mice were used for the study: senescence prone (SAMP) and senescence resistant (SAMR). Accelerated senescence refers to the tendency for SAMP mice to age more rapidly and have a 26% shorter life span than the SAMR mice (39). The fact that SAMP strains undergo accelerated senescence was concluded based on data from survival curves, Gompertzian function, growth patterns, and a specifically developed grading score. These parameters were also used to confirm that these mice underwent accelerated senescence after the developmental period was complete as opposed to premature aging. The scoring system was developed by Hosokawa and associates (39) and includes such criteria as passive and reactive behavior, skin and hair quality, eye and skin lesions, and spinal lordokyphosis . SAMP mice are particularly prone to amyloid deposition, cataracts, osteoporosis, memory loss and impaired learning, degenerative joint disease, decreased immune responses, increased lordokyphosis, and various other hallmarks of aging (11). Evidence of heightened oxidant stress

in SAMP mice includes increased lipid peroxidation early in life. Currently, there are nine SAMP strains and three SAMR strains with some phenotypic differences (11). SAMP and SAMR strains differ at multiple genetic loci from the AKR/J progenitors, probably as a result of outbreeding before the SAM strains were created (39). The SAM model is important experimentally because these mice undergo accelerated senescence without any experimental manipulation and they display most of the common age-associated disorders seen in aging humans (39).

The most common manifestation of lung pathophysiology in SAM strains is senile hyperinflation. As evidenced by an increased mean linear intercept, SAM strains showed enlargement of airspaces with increasing age that are greater and occur earlier in SAMP strains as compared with SAMR strains (40). The SAMP mice have a leftward shift in lung pressure–volume curves, indicating loss of elastic recoil, and an increased exponent *K*, an indicator of lung distensibility (40). In other morphometric studies, SAMP strains had increased lung volume, mean linear intercept, total alveolar duct air volume, and total alveolar air volume, and decreased internal surface area per unit lung volume and total elastic fiber length per unit lung volume (41). In a biochemical analysis of SAM strains, it was found that the two main contributing factors to senile alterations in lung structure and function were an impaired glutathione system and increased oxidant–antioxidant imbalance with recruitment of immune cells to the lungs (42). In studies where mice were chronically exposed to tobacco smoke, SAMP mice had increased oxygen radical generation, increased elastase-like activity, decreased glutathione, and decreased elastase inhibitory capacity, implicating increased oxidant stress as important in lung senescence (43). Other studies confirm that SAMP mice are more susceptible to damage from tobacco smoke than SAMR mice (44). The fact that SAMP mice exhibit age-dependent hyperinflation, loss of elastic recoil, and increased susceptibility to inhaled toxins, similar to age-related changes in the lungs of humans, validates this as a model of lung senescence that is relevant to human aging (41).

In conclusion, we demonstrated using SAMP that there is a decrease in the ability for lung repair after bleomycin-induced lung injury associated with age. Our data suggest that this defect is related to an alteration of the types of cells recruited to the site of injury. In particular, there was a higher number of fibroblast progenitor cells or fibrocytes, and a decrease in the ability of mesenchymal stem cells to respond to soluble actors generated by the injured lung. These observations can be important for future cell therapies using BMDMSCs in lung injury.

Funding

This research was supported by grant 1K01HL084683-01A1 from the National Heart Lung and Blood Institute, and a grant from the American Federation for Aging Research, Emory University URC 2003100 and the McKelvey Center for Lung Transplantation at Emory University.

Acknowledgments

We thank Nathalie Thorn for her technical assistance.

Correspondence

Address correspondence to Mauricio Rojas, MD, Division of Pulmonary, Allergy and Critical Care Medicine, Department of Medicine, Emory University School of Medicine, Atlanta, GA 30322. Email: mrojas@emory.edu

References

1. Golden TR, Hinerfeld DA, Melov S. Oxidative stress and aging: beyond correlation. *Aging Cell*. 2002;1:117–123.
2. Hekimi S, Guarente L. Genetics and the specificity of the aging process. *Science*. 2003;299:1351–1354.
3. Tatar M, Bartke A, Antebi A. The endocrine regulation of aging by insulin-like signals. *Science*. 2003;299:1346–1351.
4. Hasty P, Campisi J, Hoeijmakers J, van Steeg H, Vijg J. Aging and genome maintenance: lessons from the mouse? *Science*. 2003;299: 1355–1359.
5. Rafi A, Castle SC, Uyemura K, Makinodan T. Immune dysfunction in the elderly and its reversal by antihistamines. *Biomed Pharmacother*. 2003;57:246–250.
6. Edelberg JM, Tang L, Hattori K, Lyden D, Rafii S. Young adult bone marrow-derived endothelial precursor cells restore aging-impaired cardiac angiogenic function. *Circ Res*. 2002;90:E89–E93.
7. Rauscher FM, Goldschmidt-Clermont PJ, Davis BH, et al. Aging, progenitor cell exhaustion, and atherosclerosis. *Circulation*. 2003;108: 457–463.
8. Conboy IM, Conboy MJ, Wagers AJ, Girma ER, Weissman IL, Rando TA. Rejuvenation of aged progenitor cells by exposure to a young systemic environment. *Nature*. 2005;433:760–764.
9. Takeda T, Hosokawa M, Higuchi K. Senescence-accelerated mouse (SAM): a novel murine model of senescence. *Exp Gerontol*. 1997;32: 105–109.
10. Miyamoto M, Kiyota Y, Yamazaki N, et al. Age-related changes in learning and memory in the senescence-accelerated mouse (SAM). *Physiol Behav*. 1986;38:399–406.
11. Okuma Y, Nomura Y. Senescence-accelerated mouse (SAM) as an animal model of senile dementia: pharmacological, neurochemical and molecular biological approach. *Jpn J Pharmacol*. 1998;78:399–404.
12. Xu J, Mora A, Shim H, Stecenko A, Brigham KL, Rojas M. Role of the SDF-1/CXCR4 axis in the pathogenesis of lung injury and fibrosis. *Am J Respir Cell Mol Biol*. 2007;37:291–299.
13. Daniels CE, Wilkes MC, Edens M, et al. Imatinib mesylate inhibits the profibrogenic activity of TGF-beta and prevents bleomycin-mediated lung fibrosis. *J Clin Invest*. 2004;114:1308–1316.
14. Xu YD, Hua J, Mui A, O'Connor R, Grotendorst G, Khalil N. Release of biologically active TGF-beta1 by alveolar epithelial cells results in pulmonary fibrosis. *Am J Physiol Lung Cell Mol Physiol*. 2003;285:L527–L529.
15. Phillips RJ, Burdick MD, Hong K, et al. Circulating fibrocytes traffic to the lungs in response to CXCL12 and mediate fibrosis. *J Clin Invest*. 2004;114:438–446.
16. Xu J, Mora A, Shim H, Stecenko A, Brigham KL, Rojas M. Role of the SDF-1/CXCR4 axis in the pathogenesis of lung injury and fibrosis. *Am J Respir Cell Mol Biol*. 2007;37:291–299.
17. Gay SE, Kazerooni EA, Toews GB, et al. Idiopathic pulmonary fibrosis: predicting response to therapy and survival. *Am J Respir Crit Care Med*. 1998;157:1063–1072.
18. Kilburn KH, Lilis R, Anderson HA, Miller A, Warshaw RH. Interaction of asbestos, age, and cigarette smoking in producing radiographic evidence of diffuse pulmonary fibrosis. *Am J Med.* 1986;80:377–381.
19. Samuel CS, Zhao C, Bathgate RA, et al. Relaxin deficiency in mice is associated with an age-related progression of pulmonary fibrosis. *Faseb J*. 2003;17:121–123.

20. Matulionis DH. Effects of cigarette smoke generated by different smoking machines on pulmonary macrophages of mice and rats. *J Anal Toxicol*. 1984;8:187–191.
21. Rossi D, Zlotnik A. The biology of chemokines and their receptors. *Annu Rev Immunol*. 2000;18:217–242.
22. Shirozu M, Nakano T, Inazawa J, et al. Structure and chromosomal localization of the human stromal cell-derived factor 1 (SDF1) gene. *Genomics*. 1995;28:495–500.
23. Lataillade JJ, Clay D, Bourin P, et al. Stromal cell-derived factor 1 regulates primitive hematopoiesis by suppressing apoptosis and by promoting G(0)/G(1) transition in CD34(+) cells: evidence for an autocrine/paracrine mechanism. *Blood*. 2002;99:1117–1129.
24. Lee Y, Gotoh A, Kwon HJ, et al. Enhancement of intracellular signaling associated with hematopoietic progenitor cell survival in response to SDF-1/CXCL12 in synergy with other cytokines. *Blood*. 2002;99: 4307–4317.
25. Nagasawa T, Hirota S, Tachibana K, et al. Defects of B-cell lymphopoiesis and bone-marrow myelopoiesis in mice lacking the CXC chemokine PBSF/SDF-1. *Nature*. 1996;382:635–638.
26. Zou YR, Kottmann AH, Kuroda M, Taniuchi I, Littman DR. Function of the chemokine receptor CXCR4 in haematopoiesis and in cerebellar development. *Nature*. 1998;393:595–599.
27. Ara T, Tokoyoda K, Sugiyama T, Egawa T, Kawabata K, Nagasawa T. Long-term hematopoietic stem cells require stromal cell-derived factor-1 for colonizing bone marrow during ontogeny. *Immunity*. 2003;19: 257–267.
28. Ponomaryov T, Peled A, Petit I, et al. Induction of the chemokine stromal-derived factor-1 following DNA damage improves human stem cell function. *J Clin Invest*. 2000;106:1331–1339.
29. Ji JF, He BP, Dheen ST, Tay SS. Interactions of chemokines and chemokine receptors mediate the migration of mesenchymal stem cells to the impaired site in the brain after hypoglossal nerve injury. *Stem Cells*. 2004;22:415–427.
30. Wright DE, Bowman EP, Wagers AJ, Butcher EC, Weissman IL. Hematopoietic stem cells are uniquely selective in their migratory response to chemokines. *J Exp Med*. 2002;195:1145–1154.
31. Kucia M, Ratajczak J, Reca R, Janowska-Wieczorek A, Ratajczak MZ. Tissue-specific muscle, neural and liver stem/progenitor cells reside in the bone marrow, respond to an SDF-1 gradient and are mobilized into peripheral blood during stress and tissue injury. *Blood Cells Mol Dis*. 2004;32:52–57.
32. Schober A, Knarren S, Lietz M, Lin EA, Weber C. Crucial role of stromal cell-derived factor-1alpha in neointima formation after vascular injury in apolipoprotein E-deficient mice. *Circulation*. 2003;108:2491–2497.
33. Abbott JD, Huang Y, Liu D, Hickey R, Krause DS, Giordano FJ. Stromal cell-derived factor-1alpha plays a critical role in stem cell recruitment to the heart after myocardial infarction but is not sufficient to induce homing in the absence of injury. *Circulation*. 2004;110: 3300–3305.
34. Yamaguchi J, Kusano KF, Masuo O, et al. Stromal cell-derived factor-1 effects on ex vivo expanded endothelial progenitor cell recruitment for ischemic neovascularization. *Circulation*. 2003;107:1322–1328.
35. Ceradini DJ, Kulkarni AR, Callaghan MJ, et al. Progenitor cell trafficking is regulated by hypoxic gradients through HIF-1 induction of SDF-1. *Nat Med*. 2004;10:858–864.
36. Askari AT, Unzek S, Popovic ZB, et al. Effect of stromal-cell-derived factor 1 on stem-cell homing and tissue regeneration in ischaemic cardiomyopathy. *Lancet*. 2003;362:697–703.
37. Kollet O, Shivtiel S, Chen YQ, et al. HGF, SDF-1, and MMP-9 are involved in stress-induced human CD34+ stem cell recruitment to the liver. *J Clin Invest*. 2003;112:160–169.
38. Heissig B, Hattori K, Dias S, et al. Recruitment of stem and progenitor cells from the bone marrow niche requires MMP-9 mediated release of kit-ligand. *Cell*. 2002;109:625–637.
39. Hosokawa M, Abe T, Higuchi K, et al. Management and design of the maintenance of SAM mouse strains: an animal model for accelerated senescence and age-associated disorders. *Exp Gerontol*. 1997;32: 111–116.
40. Teramoto S, Fukuchi Y, Uejima Y, Teramoto K, Oka T, Orimo H. A novel model of senile lung: senescence-accelerated mouse (SAM). *Am J Respir Crit Care Med*. 1994;150:238–234.
41. Kurozumi M, Matsushita T, Hosokawa M, Takeda T. Age-related changes in lung structure and function in the senescence-accelerated mouse (SAM): SAM-P/1 as a new murine model of senile hyperinflation of lung. *Am J Respir Crit Care Med*. 1994;149:776–782.
42. Teramoto S, Fukuchi Y, Uejima Y, Teramoto K, Orimo H. Biochemical characteristics of lungs in senescence-accelerated mouse (SAM). *Eur Respir J*. 1995;8:450–456.
43. Uejima Y, Fukuchi Y, Nagase T, Tabata R, Orimo H. A new murine model of aging lung: the senescence accelerated mouse (SAM)-P. *Mech Ageing Dev*. 1991;61:223–236.
44. Teramoto S, Fukuchi Y, Uejima Y, Teramoto K, Orimo H. Influences of chronic tobacco smoke inhalation on aging and oxidant-antioxidant balance in the senescence-accelerated mouse (SAM)-P/2. *Exp Gerontol*. 1993;28:87–95.

Received December 5, 2008
Accepted February 25, 2009
Decision Editor: Huber R. Warner, PhD